Supporting Information for

Activation of C-H Bonds in $Pt^+ + xCH_4$ Reactions, where $x = 1 – 4$: Identification of the Platinum Dimethyl Cation

Oscar W. Wheeler,[†] Michelle Salem,[†,‡] Amanda Gao,[†,ǁ] Joost M. Bakker,[§] and P. B. Armentrout[*,†]

[†]*Department of Chemistry, University of Utah, 315 S. 1400 E. Room 2020, Salt Lake City, Utah 84112, United States*

[‡]*Present address: Department of Chemistry and Biochemistry, California State University San Marcos, 333 S. Twin Oaks Valley Rd., San Marcos, California 92096, United States*

[ǁ]*Present address: Department of Chemistry and Chemical Engineering, California Institute of Technology, 1200 E. California Boulevard, Pasedena, California 91125, United States*

[§]*Radboud University, Institute for Molecules and Materials, FELIX Laboratory, Toernooiveld 7c, 6525ED Nijmegen, The Netherlands*

Table S1. Theoretical thermochemistry (in eV) for the potential energy surface of Pt^+ reacting with CH_4

	MP2(full)[a]	B3LYP[a,b]	B3LYP						PCI-80[e]
structure	def2	def2	def2[a]	TZ-HW[c]	TZ-HW+[c]	TZ-HW+X[c]	TZ-SD[d]	DZ-HWX[e]	
$Pt^+ + CH_4$	0.00	0.00	0.00	0.00	0.00	0.00	0.00	0.00	0.00
$PtCH_4^+$ (**1**')	-1.60	-1.31	-1.35	-0.92	-0.85	-0.90	-1.31	-0.83	-1.10
TS1/2'	-1.56	-1.21	-1.08	-0.83	-0.73	-0.81	-1.29	-0.92	-1.18
$HPtCH_3^+$ (**2'**)	-2.31	-1.58	-1.46	-1.57	-1.49	-1.58	-1.76	-1.59	-1.68
TS2/3'	-1.58	-0.97	-0.83	-0.52	-0.42	-0.55	-0.74	-0.46	-0.62
$(H)_2PtCH_2^+$ (**3'**)	-1.80	-1.18	-1.05	-0.75	-0.65	-0.78	-0.96	-0.67	-0.74
TS3/4'	-1.44	-0.92	-0.79	-0.42	-0.32	-0.48	-0.68	-0.28	-0.28
$(H_2)PtCH_2^+$(**4'**)	-1.26	-1.06	-0.95	-0.58	-0.51	-0.65	-0.84	-0.68	-0.72
$PtCH_2^+ + H_2$	-0.59	-0.43	-0.37	-0.06	0.04	0.06	-0.26	-0.04	-0.18

[a] Present results calculated using def2-TZVPPD basis set and B3LYP/def2-TZVPPD geometry optimizations and zero point energy corrections. [b] Geometry optimizations performed with empirical dispersion corrections (GD3BJ) to the B3LYP level of theory. [c] Ref. 1. [d] Ref. 2. [e] Ref. 3.

(1) Zhang, X.-G.; Liyanage, R.; Armentrout, P. B., The Potential Energy Surface for Activation of Methane by Pt^+: A Detailed Guided-Ion Beam Study. *J. Am. Chem. Soc.* **2001,** *123*, 5563-5575.

(2) Achatz, U.; Beyer, M.; Joos, S.; Fox, B. S.; Niedner-Schatteburg, G.; Bondybey, V. E., The Platinum Hydrido-Methyl Complex: A Frozen Reaction Intermediate? *J. Phys. Chem. A* **1999,** *103*, 8200-8206.

(3) Pavlov, M.; Blomberg, M. R. A.; Siegbahn, P. E. M.; Wesendrup, R.; Heinemann, C.; Schwarz, H., Pt^+-Catalyzed Oxidation of Methane: Theory and Experiment. *J. Phys. Chem. A* **1997,** *101*, 1567-1579.

Table S2. Thermochemistry for the potential energy surface of $HPtCH_3^+$ reacting with CH_4

species	B3LYP (eV)[a]
$HPtCH_3^+ + CH_4$	0.00
$HPt(CH_3)(CH_4)^+$ (**7**)	-0.58
TS7/8	0.16
$(H)_2Pt(CH_3)_2^+$ (**8**)	0.01
TS8/9	0.15
$(H_2)Pt(CH_3)_2^+$ (**9**)	-0.12
$Pt(CH_3)_2^+ + H_2$	0.51
TS9/5	1.70
$PtC_2H_6^+$_bod (**5**) + H_2	0.94
TS5/6	0.97
$PtC_2H_6^+$_end (**6**) + H_2	0.92
$Pt^+ + C_2H_6 + H_2$	2.54

[a] Energies from B3LYP/def2-TZVPPD level of theory including zero point energy corrections.

Figure Captions

Figure S1. Frequency calculations of the $Pt(CH_3)_2^+(CH_4)_2$_cis species for the listed level of theory and basis set. Part a shows B3LYP/def2-SVP vibrational frequencies scaled by 0.983. Part b shows the B3LYP/def2-TZVPPD vibrational spectrum in blue with GD3BJ dispersion corrections in red. Part c shows B3LYP/mDZP/def2-TZVPPD frequencies in green with B3LYP-GD3BJ/mDZP/def2-TZVPPD results in red. Part d shows scaled frequencies for B3LYP geometry optimizations with the 3 different basis sets.

Figure S2. Part a shows mass scans both with (red) and without (black) FELIX at ~1195 cm^{-1}. Part b represents the change in signal for the m/z 209 channel associated with the $[^{195}Pt,C,2H]^+$ product with (red) and without (black) FELIX. Products appearing at 208, 209, 210, and 212 *m/z* correspond to the major isotopes, 194 (33 %), 195 (34 %), 196 (25 %), and 198 (7 %), of Pt with an attached CH_2 group.

Figure S3. All $[Pt,2C,6H]^+$ structures examined in the current work optimized at the B3LYP/def2 level of theory.

Figures S4 and S5. Experimental spectra for $[Pt,4C,14H/D]^+$ and $[Pt,3C,10H/D]^+$ graphed against spectra generated from B3LYP calculations with def2-SVP, def2-TZVPPD, and mDZP/def2-TZVPPD basis sets. A scaling factor of 0.983 was used for both def2 basis sets and 1.0 for the mDZP basis set.

Figure S6. IRMPD depletion yield spectrum, $-\ln (I_{sig}/I_{ref})$, for $[Pt,4C,14H/D]^+$ (top and in shade) and below that the B3LYP/def2-TZVPPD calculated spectra for two isomers not included in Figure 2.

Figure S7. IRMPD depletion yield spectrum, -ln (I_{sig}/I_{ref}), for $[Pt,3C,10H/D]^+$ (top and in shade) and below that the B3LYP/def2-TZVPPD calculated spectra for two isomers not included in Figure 3.

Figure S8. Potential energy surface for the reaction of $Pt^+ + CH_4$ from the current work and select literature references. All theoretical values are listed in Table S1. Solid red circles with error bars represent the experimental results from the GIBMS study, Ref. 1, for the $HPtCH_3^+$ well depth and $PtCH_2^+ + H_2$ exothermicity.

Figure S9. Structures of intermediates and transition states found in Figure S8 calculated at the B3LYP/def2-TZVPPD level of theory.

Figure S10. Potential energy surface for the reaction of $PtCH_2^+ + CH_4$ expanded to include alternative pathways for formation of a C-C bond.

Figure S11. Potential energy surface for the reaction of $HPtCH_3^+ + CH_4$. Relative energies are calculated at the B3LYP/def2-TZVPPD level of theory and are listed in Table S2.

Figure S12. B3LYP/def2-TZVPPD structures for species shown in Figure S11. Transition states include the imaginary frequency in cm^{-1}.

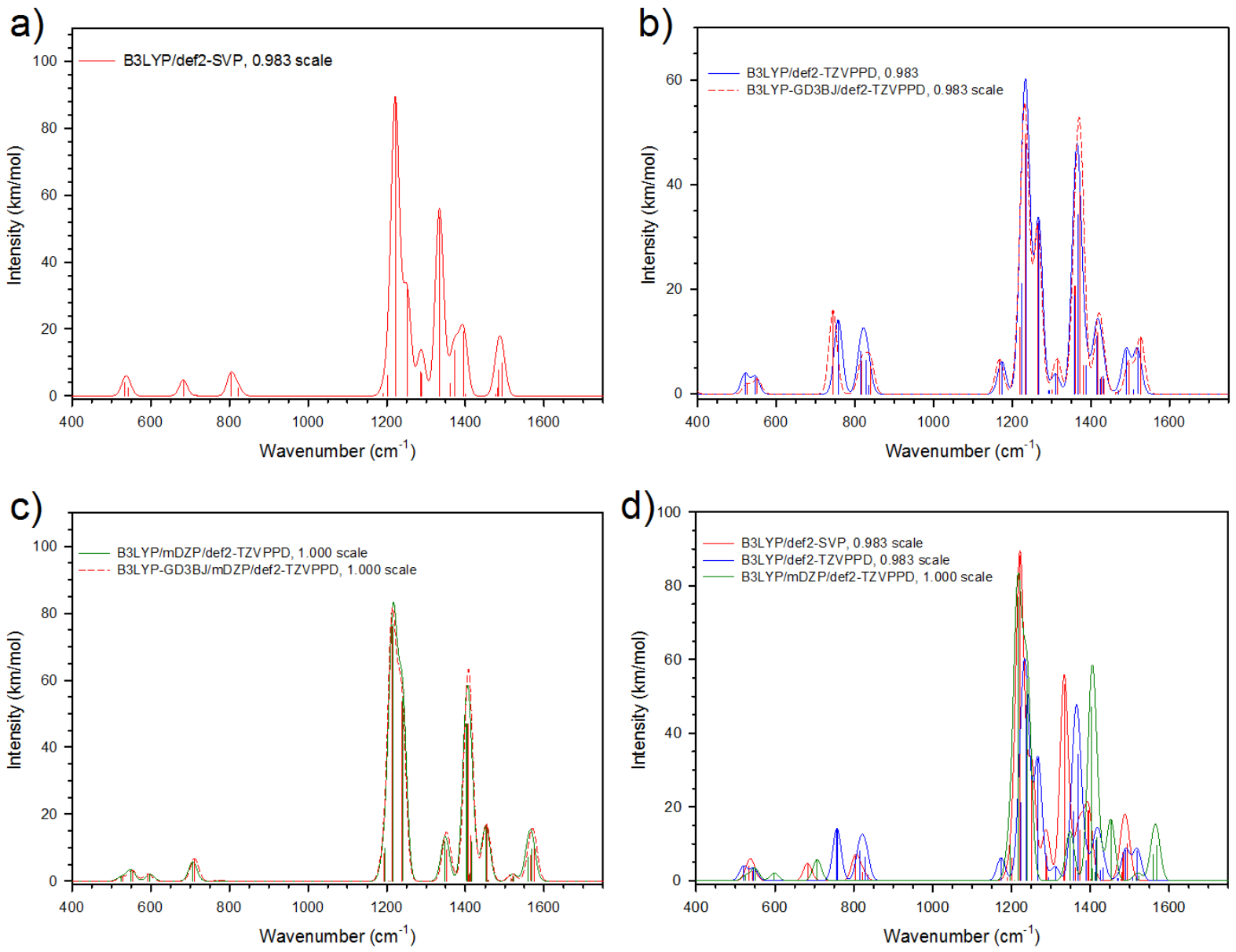
a)
B3LYP/def2-SVP, 0.983 scale
Intensity (km/mol)
Wavenumber (cm-1)
b)
B3LYP/def2-TZVPPD, 0.983
B3LYP-GD3BJ/def2-TZVPPD, 0.983 scale
Intensity (km/mol)
Wavenumber (cm-1)
c)
B3LYP/mDZP/def2-TZVPPD, 1.000 scale
B3LYP-GD3BJ/mDZP/def2-TZVPPD, 1.000 scale
Intensity (km/mol)
Wavenumber (cm-1)
d)
B3LYP/def2-SVP, 0.983 scale
B3LYP/def2-TZVPPD, 0.983 scale
B3LYP/mDZP/def2-TZVPPD, 1.000 scale
Intensity (km/mol)
Wavenumber (cm-1)

Figure S1

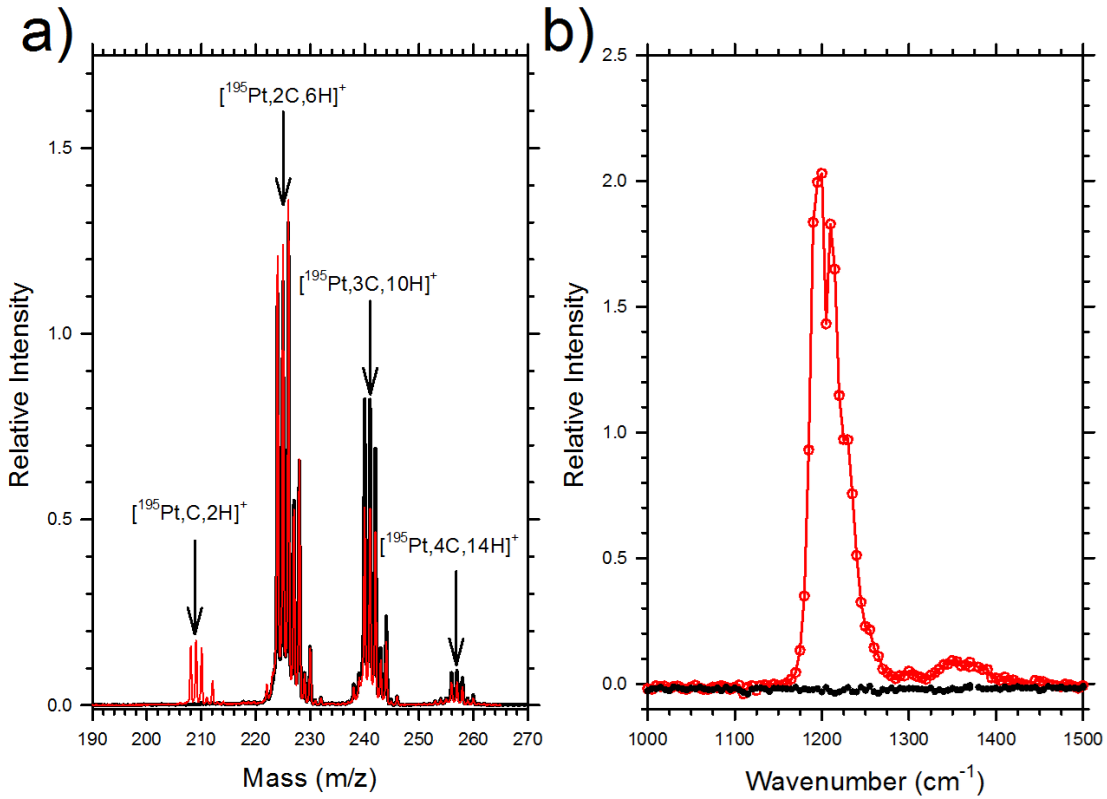
a)
b)
[195Pt,2C,6H]+
[195Pt,3C,10H]+
[195Pt,C,2H]+
[195Pt,4C,14H]+
Relative Intensity
Mass (m/z)
Wavenumber (cm-1)

Figure S2

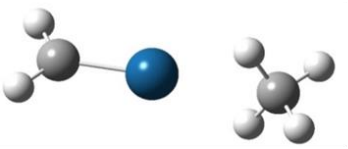

$(CH_4)PtCH_2^+$ ($^2A'$) (**1**)

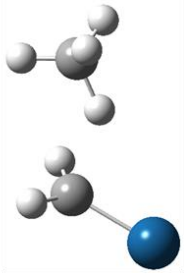

$PtCH_2^+(CH_4)$ (^2A) (**1***)

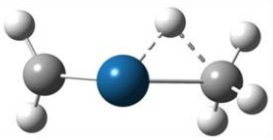

TS1/2 (^2A) *i -838* cm^{-1}

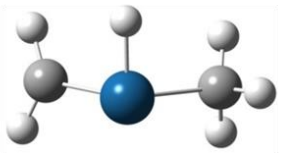

$HPtCH_2(CH_3)^+$ (^2A) (**2**)

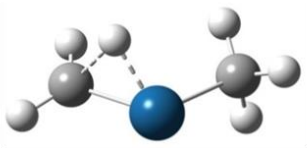

TS2/3 (^2A) *i -816* cm^{-1}

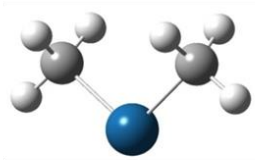

$Pt(CH_3)_2^+$ (^2A) (**3**)

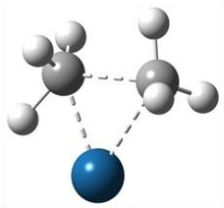

TS3/5 (^2A) *i -508* cm^{-1}

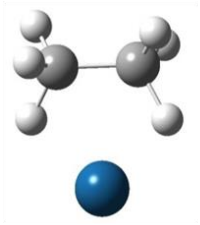

$Pt^+(C_2H_6)$ _bod (^2A) (**5**)

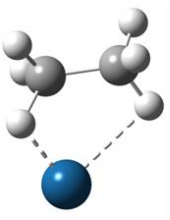

TS5/6 (^2A) *i -161* cm^{-1}

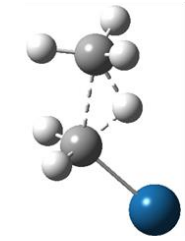

TS1*/6 (^2A) *i -393* cm^{-1}

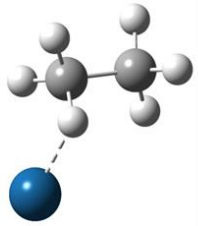

$Pt^+(C_2H_6)$ _end (^2A) (**6**)

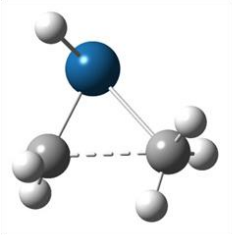

TS2/4 (^2A) *i -362* cm^{-1}

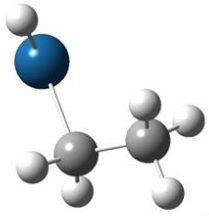

$HPtC_2H_5^+$ (^2A) (**4**)

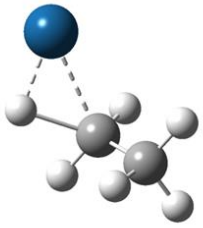

TS4/6 (^2A) *i -745* cm^{-1}

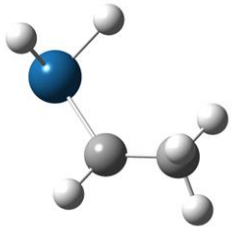

$H_2PtCHCH_3^+$ (^2A)

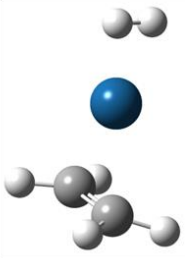

$(H_2)Pt(C_2H_4)^+$ (^2A)

Figure S3

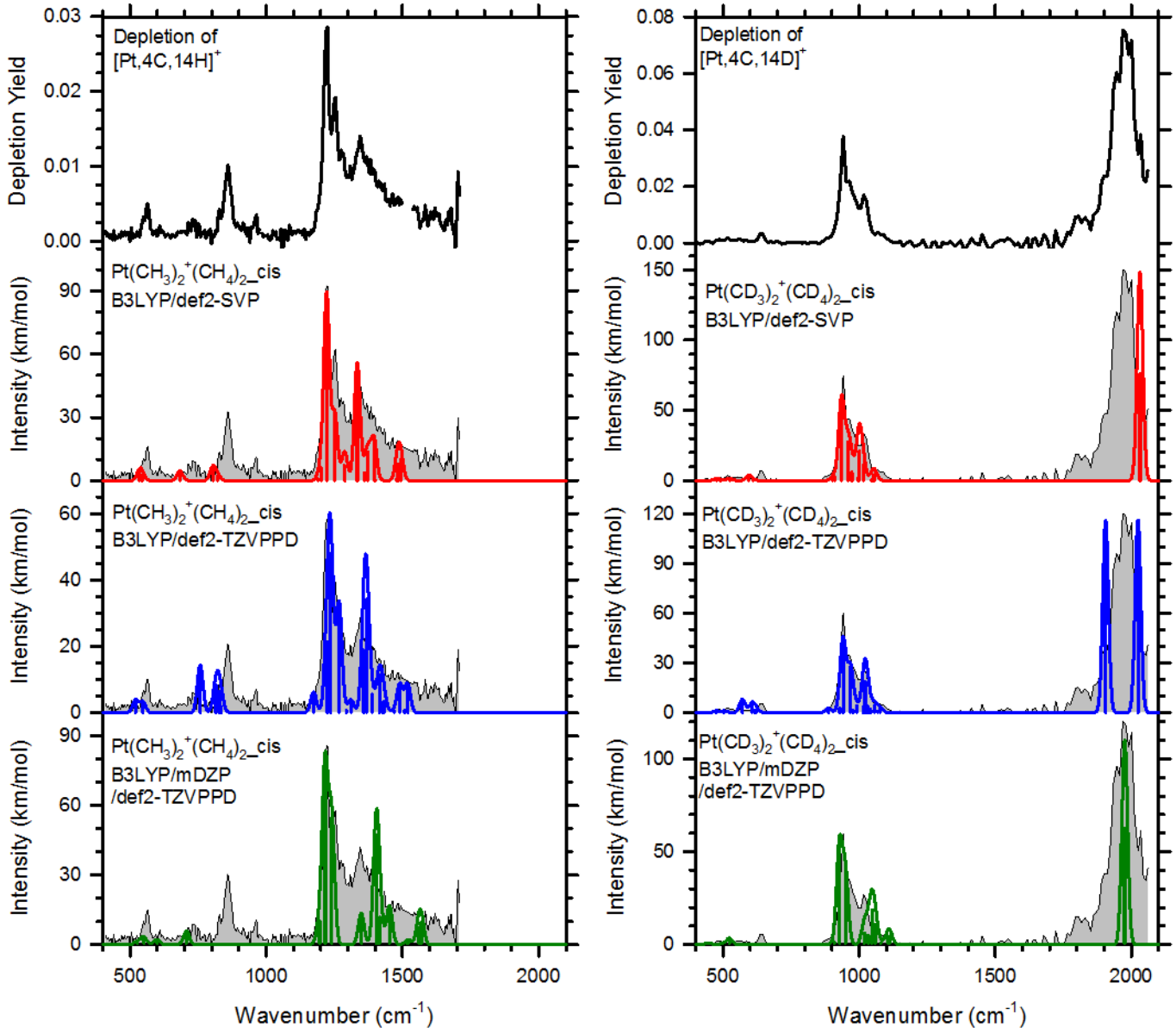
Depletion of
[Pt,4C,14H]+
Depletion Yield
Pt(CH3)2+(CH4)2_cis
B3LYP/def2-SVP
Intensity (km/mol)
Pt(CH3)2+(CH4)2_cis
B3LYP/def2-TZVPPD
Intensity (km/mol)
Pt(CH3)2+(CH4)2_cis
B3LYP/mDZP
/def2-TZVPPD
Intensity (km/mol)
Wavenumber (cm-1)
Depletion of
[Pt,4C,14D]+
Depletion Yield
Pt(CD3)2+(CD4)2_cis
B3LYP/def2-SVP
Intensity (km/mol)
Pt(CD3)2+(CD4)2_cis
B3LYP/def2-TZVPPD
Intensity (km/mol)
Pt(CD3)2+(CD4)2_cis
B3LYP/mDZP
/def2-TZVPPD
Intensity (km/mol)
Wavenumber (cm-1)

Figure S4

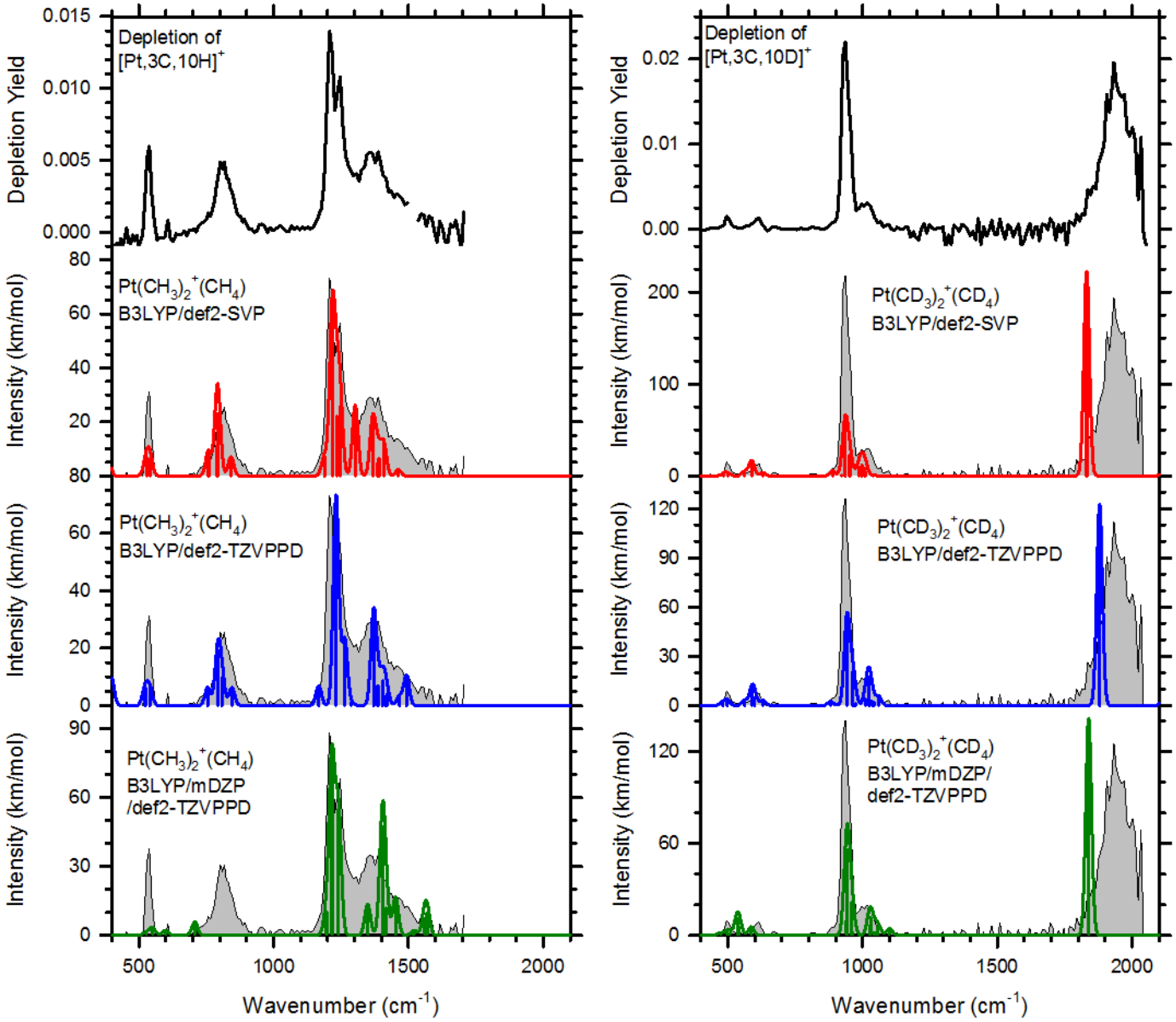
Depletion of
[Pt,3C,10H]+
Depletion Yield
Pt(CH3)2+(CH4)
B3LYP/def2-SVP
Pt(CH3)2+(CH4)
B3LYP/def2-TZVPPD
Pt(CH3)2+(CH4)
B3LYP/mDZP
/def2-TZVPPD
Intensity (km/mol)
Wavenumber (cm-1)
Depletion of
[Pt,3C,10D]+
Pt(CD3)2+(CD4)
B3LYP/def2-SVP
Pt(CD3)2+(CD4)
B3LYP/def2-TZVPPD
Pt(CD3)2+(CD4)
B3LYP/mDZP/
def2-TZVPPD

Figure S5

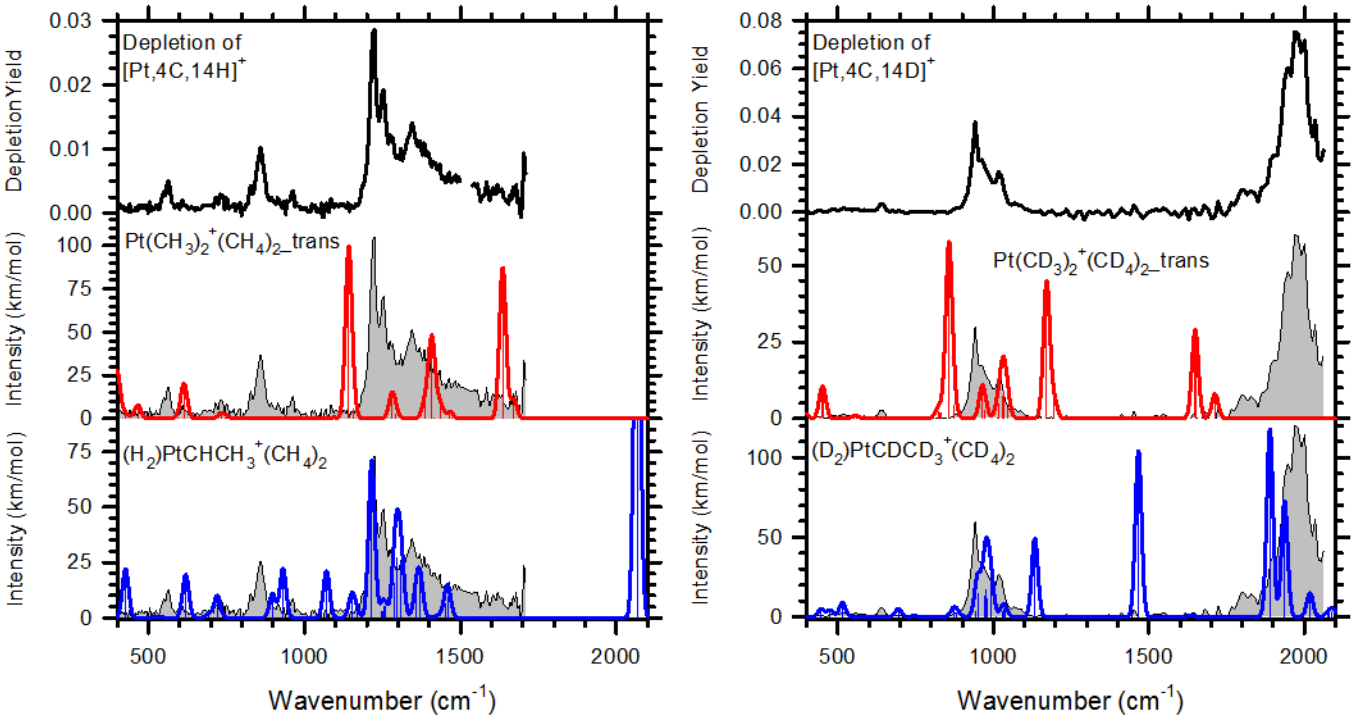
Depletion of
[Pt,4C,14H]+
Depletion Yield
Pt(CH3)2+(CH4)2_trans
Intensity (km/mol)
(H2)PtCHCH3+(CH4)2
Intensity (km/mol)
Wavenumber (cm-1)
Depletion of
[Pt,4C,14D]+
Depletion Yield
Pt(CD3)2+(CD4)2_trans
Intensity (km/mol)
(D2)PtCDCD3+(CD4)2
Intensity (km/mol)
Wavenumber (cm-1)

Figure S6

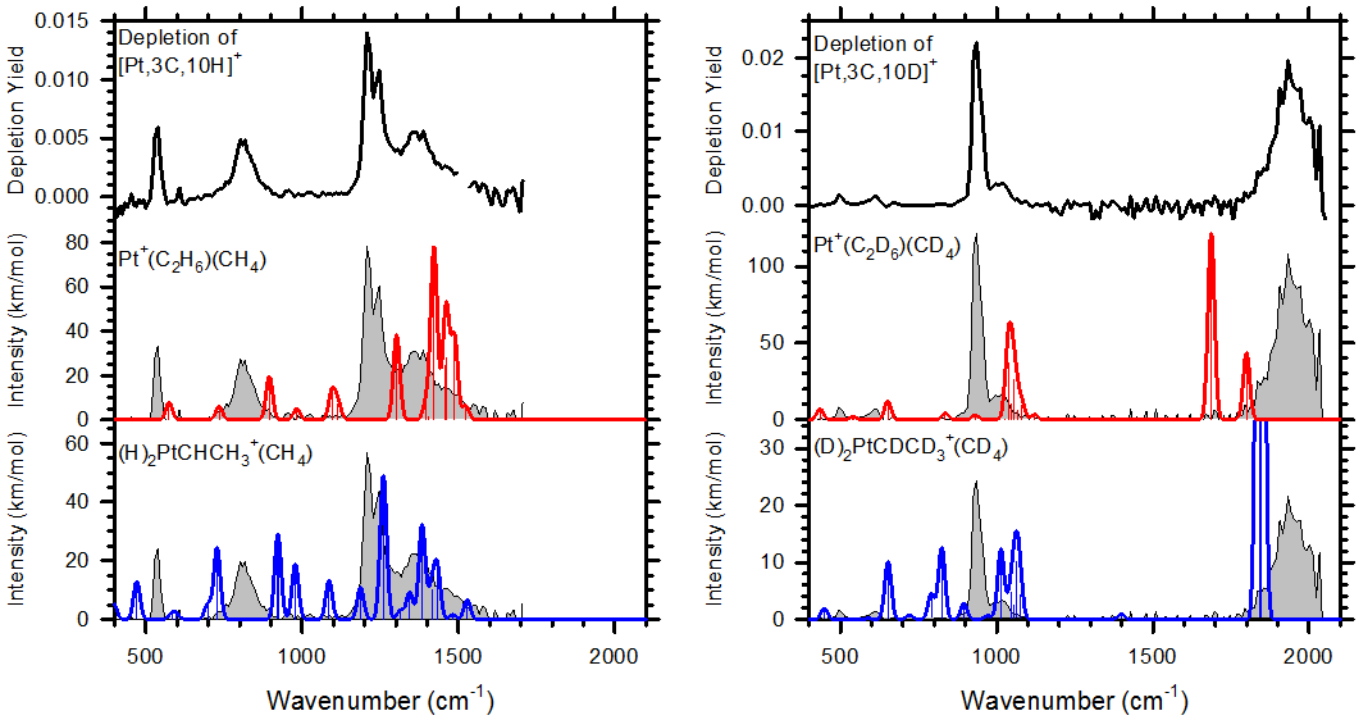
Depletion of
[Pt,3C,10H]+
Depletion Yield
Pt+(C2H6)(CH4)
Intensity (km/mol)
(H)2PtCHCH3+(CH4)
Intensity (km/mol)
Wavenumber (cm-1)
Depletion of
[Pt,3C,10D]+
Depletion Yield
Pt+(C2D6)(CD4)
Intensity (km/mol)
(D)2PtCDCD3+(CD4)
Intensity (km/mol)
Wavenumber (cm-1)

Figure S7

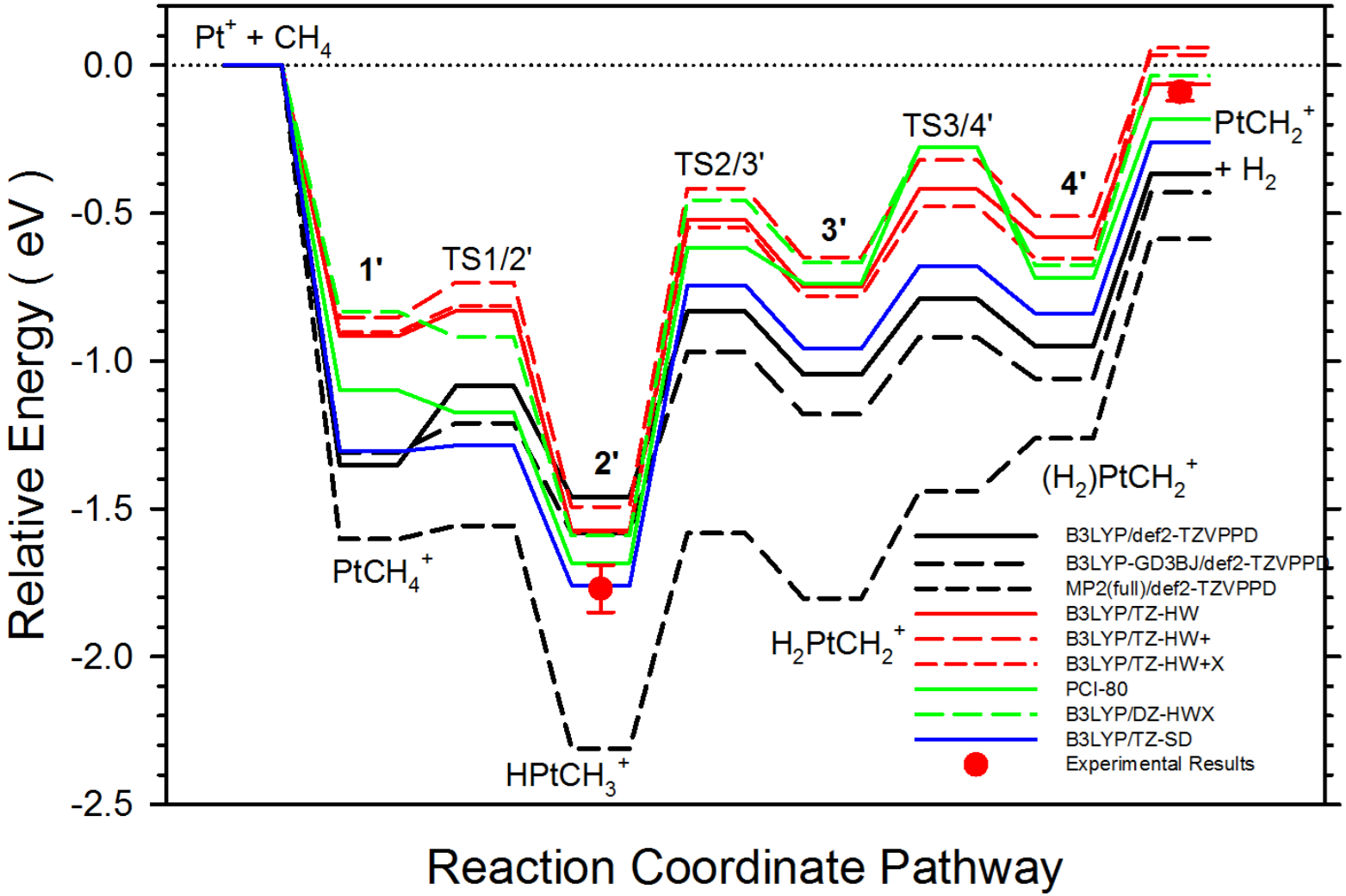
Pt+ + CH4
0.0
-0.5
-1.0
-1.5
-2.0
-2.5
Relative Energy (eV)
1'
TS1/2'
2'
TS2/3'
3'
TS3/4'
4'
PtCH2+
+ H2
(H2)PtCH2+
PtCH4+
HPtCH3+
H2PtCH2+
B3LYP/def2-TZVPPD
B3LYP-GD3BJ/def2-TZVPPD
MP2(full)/def2-TZVPPD
B3LYP/TZ-HW
B3LYP/TZ-HW+
B3LYP/TZ-HW+X
PCI-80
B3LYP/DZ-HWX
B3LYP/TZ-SD
Experimental Results
Reaction Coordinate Pathway

Figure S8

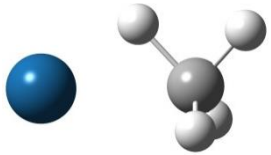

$Pt^{+}(CH_4)$ (^{2}A') (**1'**)

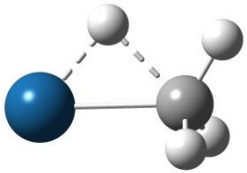

TS1/2 (^{2}A) *i -790* cm^{-1}

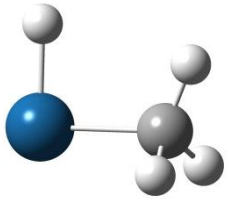

$HPtCH_3^{+}$ (^{2}A') (**2'**)

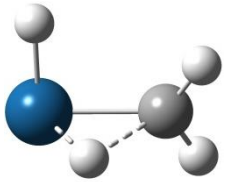

TS2/3 (^{2}A) *i -794* cm^{-1}

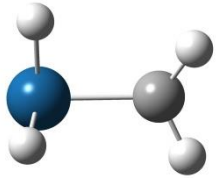

$H_2PtCH_2^{+}$ (^{2}A) (**3'**)

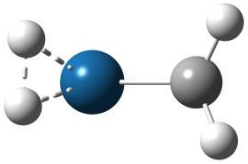

TS3/4 (^{2}A) *i -704* cm^{-1}

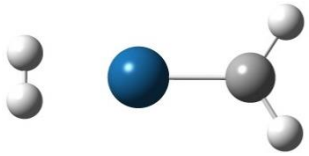

$(H_2)PtCH_2^{+}$ (^{2}A') (**4'**)

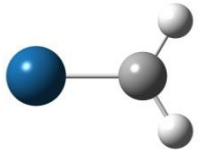

$PtCH_2^{+}$ ($^2A_1$)

Figure S9

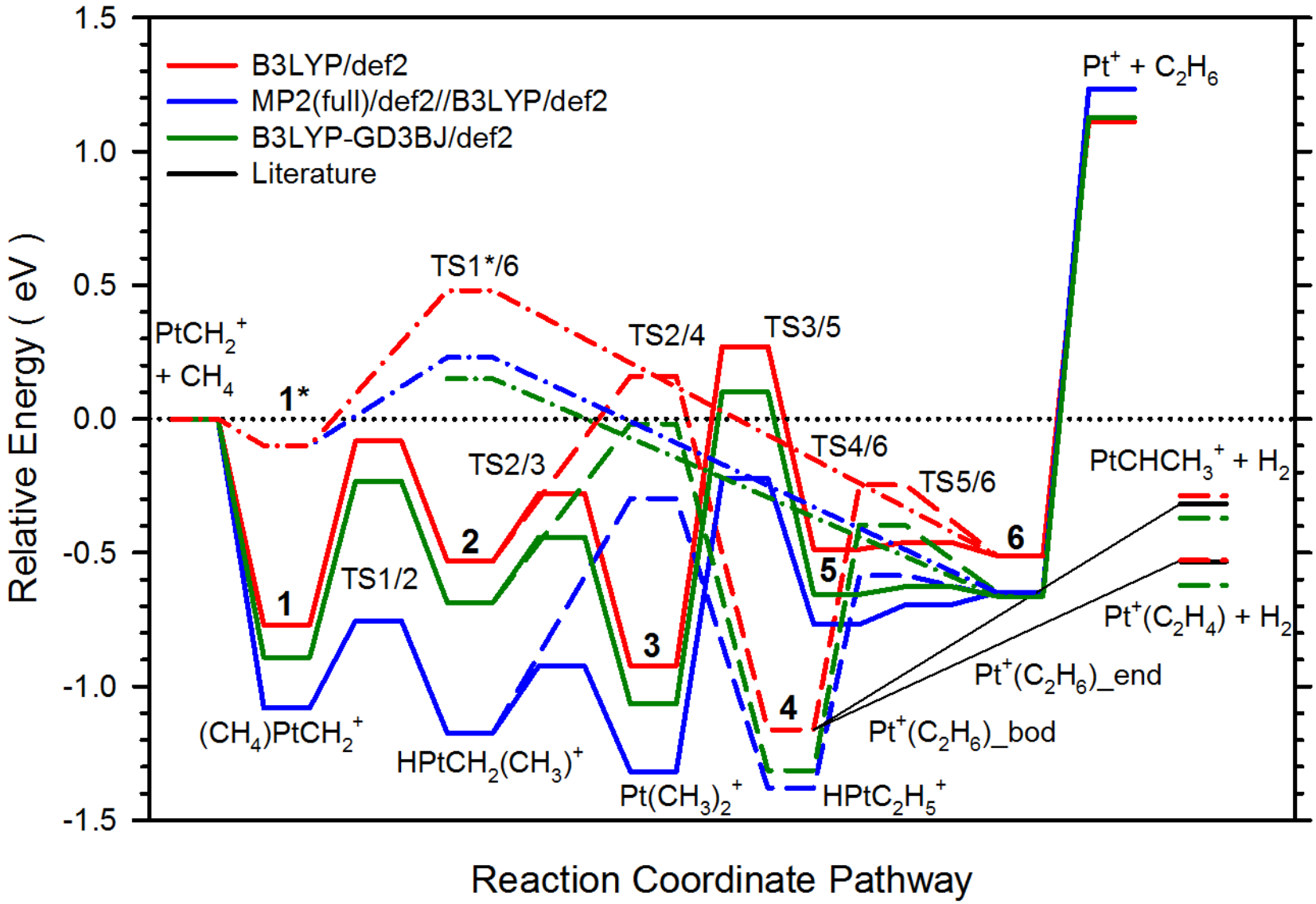
B3LYP/def2
MP2(full)/def2//B3LYP/def2
B3LYP-GD3BJ/def2
Literature
Relative Energy (eV)
Reaction Coordinate Pathway
1.5
1.0
0.5
0.0
-0.5
-1.0
-1.5
PtCH2+ + CH4
1*
TS1*/6
TS2/4
TS3/5
TS4/6
TS5/6
TS2/3
TS1/2
1
2
3
4
5
6
(CH4)PtCH2+
HPtCH2(CH3)+
Pt(CH3)2+
HPtC2H5+
Pt+ + C2H6
PtCHCH3+ + H2
Pt+(C2H4) + H2
Pt+(C2H6)_end
Pt+(C2H6)_bod

Figure S10

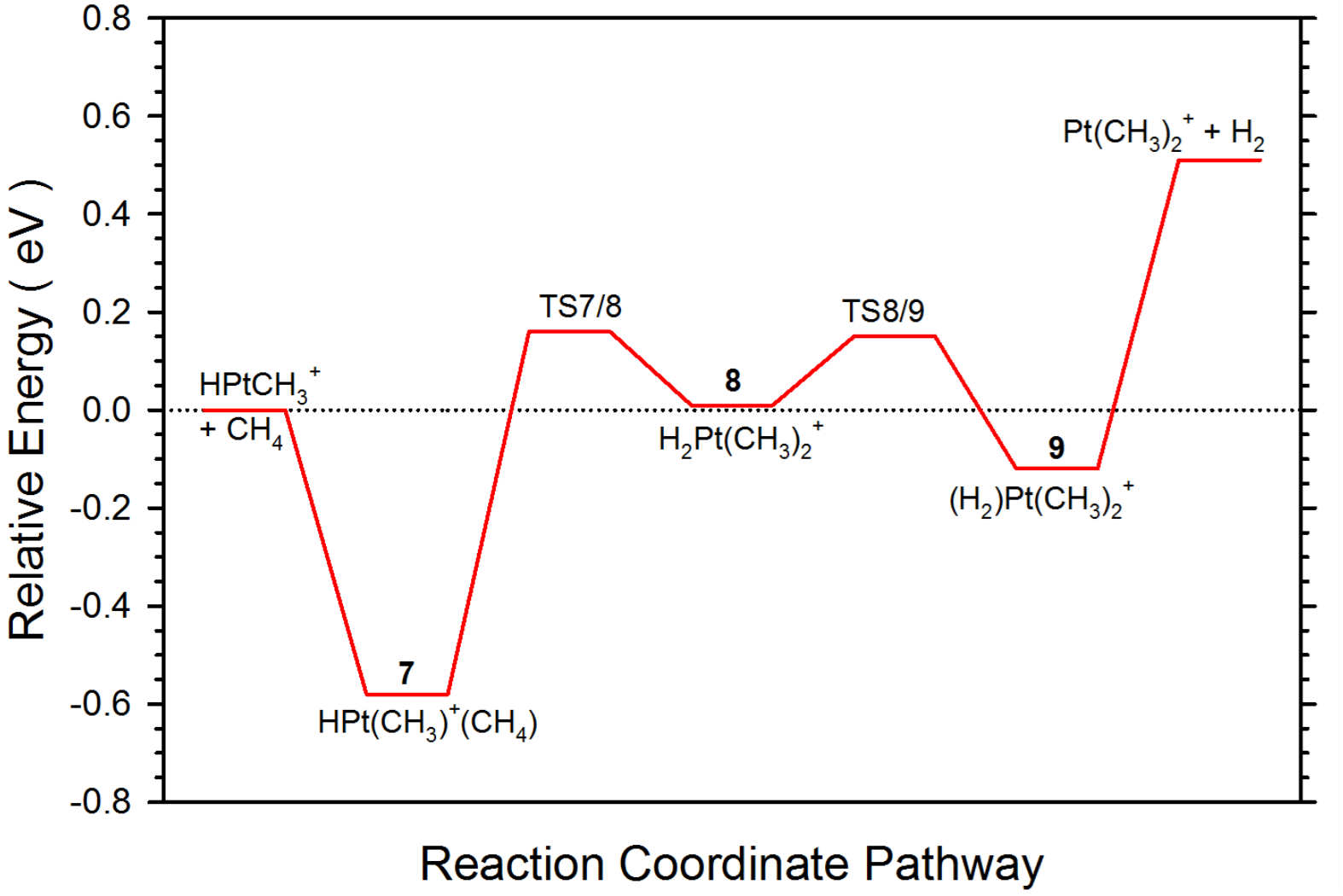
0.8
0.6
0.4
0.2
0.0
-0.2
-0.4
-0.6
-0.8
Relative Energy (eV)
HPtCH3+
+ CH4
7
HPt(CH3)+(CH4)
TS7/8
8
H2Pt(CH3)2+
TS8/9
9
(H2)Pt(CH3)2+
Pt(CH3)2+ + H2
Reaction Coordinate Pathway

Figure S11

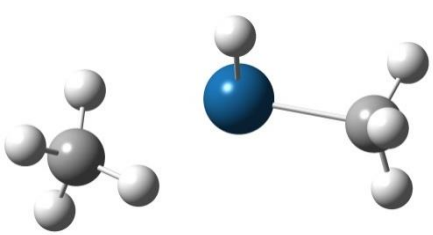

$HPtCH_3^+(CH_4)$ (^2A) (**7**)

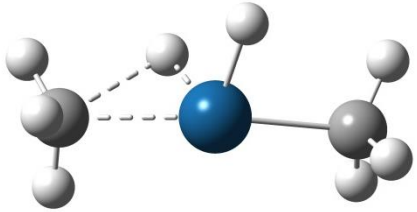

TS6/7 (^2A) *i -686* cm^{-1}

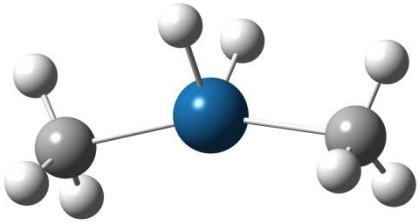

$H_2Pt(CH_3)_2^+$ (^2A) (**8**)

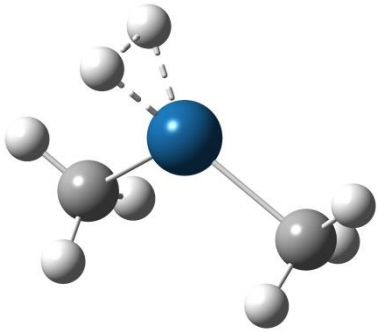

TS7/8 (^2A) *i -863* cm^{-1}

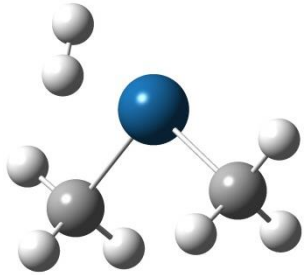

$(H_2)Pt(CH_3)_2^+$ (^2A) (**9**)

Figure S12